

pubs.acs.org/JACS Article

Expanded [23]-Helicene with Exceptional Chiroptical Properties via an Iterative Ring-Fusion Strategy

Gavin R. Kiel, Harrison M. Bergman, Adrian E. Samkian, Nathaniel J. Schuster, Rex C. Handford, August J. Rothenberger, Rafael Gomez-Bombarelli, Colin Nuckolls, and T. Don Tilley*



Cite This: J. Am. Chem. Soc. 2022, 144, 23421-23427



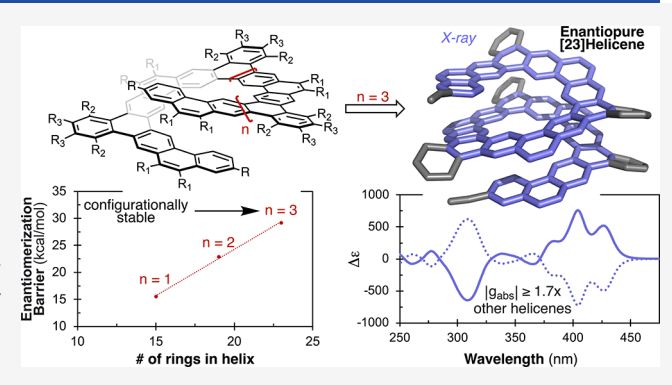
ACCESS I

III Metrics & More

Article Recommendations

sı Supporting Information

ABSTRACT: Expanded helicenes are an emerging class of helical nanocarbons composed of alternating linear and angularly fused rings, which give rise to an internal cavity and a large diameter. The latter is expected to impart exceptional chiroptical properties, but low enantiomerization free energy barriers ($\Delta G_{\rm e}^{\dagger}$) have largely precluded experimental interrogation of this prediction. Here, we report the syntheses of expanded helicenes containing 15, 19, and 23 rings on the inner helical circuit, using two iterations of an Ircatalyzed, site-selective [2 + 2 + 2] reaction. This series of compounds displays a linear relationship between the number of rings and $\Delta G_{\rm e}^{\ddagger}$. The expanded [23]-helicene, which is 7 rings longer than any known single carbohelicene and among the longest known all-carbon ladder oligomers, exhibits a $\Delta G_{\rm e}^{\ddagger}$ that is high



enough (29.2 \pm 0.1 kcal/mol at 100 °C in o-DCB) to halt enantiomerization at ambient temperature. This enabled the isolation of enantiopure samples displaying circular dichroism dissymmetry factors of \pm 0.056 at 428 nm, which are \geq 1.7× larger than values for previously reported classical and expanded helicenes. Computational investigations suggest that this improved performance is the result of both the increased diameter and length of the [23]-helicene, providing guiding design principles for high dissymmetry molecular materials.

INTRODUCTION

Helicenes are the prototypical chiral aromatic molecules that have been the subject of intense investigation for over 60 years. 1-5 This prolonged interest has been driven by the inherent structural beauty and synthetic challenge associated with these compounds, as well as a desire to establish fundamental knowledge of molecular chirality and intramolecular π -overlap. In recent years, the structural diversity of helicenes has significantly broadened, and such compounds can adopt highly complex three-dimensional shapes with multiple stereogenic elements. 6-14 Much of this heightened interest results from the new set of properties that emerge from their chirality and nonplanarity.⁵ Perhaps most notably, helicenes exhibit exceptional chiroptical properties (e.g., electronic circular dichroism (ECD) and circularly polarized luminescence), 15-19 nonlinear optical behavior, 20 novel supramolecular^{21,22} and solid-state⁸ chemistry, and high solubility. As a result, there are many new possibilities for applications in diverse areas such as catalysis²³ and (opto)electronics. ^{16,24–27}

In 2017, the Tilley group introduced a broad new class of helicenes—the "expanded helicenes" (Figure 1a)—that have an internal cavity and a larger diameter than typical carbohelicenes due to an alternation of linear and angular ring-fusion.²⁸ The structures of these compounds are much

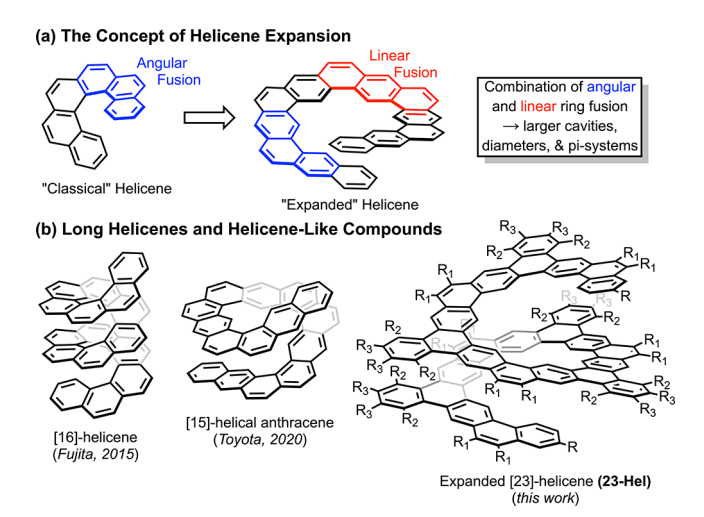


Figure 1. Overview of long and expanded helicenes.

Received: September 7, 2022 Published: December 16, 2022





more flexible than those of most other helical aromatics, which has exciting implications for their supramolecular and solidstate chemistry. For example, they can accommodate large changes in helical pitch, which has led to a remarkable doublehelical dimer driven by π -stacking interactions and a range of other higher-order structures. ^{28,29,44} This flexibility may also enable unique applications that require dynamic chirality (e.g., switchable catalysts). Unfortunately, this has also significantly impeded the isolation of enantioenriched samples and the subsequent study of their chiroptical properties.

Theoretical studies suggest that expanded helicenes should exhibit superior chiroptical properties (e.g., ECD dissymmetry factors) compared to those for helicenes with a smaller diameter.³⁰ Thus, to interrogate this hypothesis, strategies to increase the enantiomerization free energy barriers $(\Delta G^{\ddagger}_{e})$ of expanded helicenes are of tremendous interest. The Tilley group recently reported a "covalent locking" strategy whereby bridging the termini of the helicene with a phenylene unit increased its ΔG^{\ddagger}_{e} by more than 10 kcal/mol relative to its nonbridged precursor.²⁹ Unfortunately, the ΔG_e^{\ddagger} magnitude (22 kcal/mol at 25 °C) is still too low to prevent rapid racemization at room temperature. Additionally, the Toyota group employed a "noncovalent locking" approach on a subclass of expanded helicenes they called "helical anthracenes."31 Bulky phenyl rings were incorporated on the inner edge for a nine-ring congener, which raised ΔG^{\ddagger} to 28.9 kcal/ mol at 90 °C and enabled the separation of enantiomers. This compound displayed a maximum CD dissymmetry factor, $|g_{abs}|$, of 0.024 at 352 nm, supporting the theory that expanded helicenes should display superior chiroptical properties. Yashima and co-workers have shown that fusing multiple helical anthracenes together also effectively enables the separation of enantiomers, but these multiple helicenes display inferior $|g_{abs}|$ of ≤ 0.015 . Notably, the original expanded helicenes illustrated in Figure 1a have larger diameters than helical anthracenes (\sim 13.5 vs \sim 11.5 Å), suggesting that they should show further improvement in $|g_{abs}|$; however, a similar noncovalent locking strategy was attempted on such an expanded helicene that failed to provide configurational stability.33

Lengthening the helicene backbone also increases ΔG^{\ddagger}_{e} , but this poses a considerable synthetic challenge. Since Newman's landmark synthesis of [6] helicene in 1956, 34 there has been significant effort devoted to this challenge. Figure 1b shows the longest classical and expanded helicenes synthesized to date. Until Fujita's synthesis of [16]helicene in 2015, 35 the previous record length for a carbohelicene (14 rings 36) stood for 40 years. In 2020, Toyota reported a [15]helical anthracene, but due to its conformational flexibility, it could not be isolated in the enantiopure form.³⁷ Thus, the synthesis of even longer oligomers will be necessary to apply this strategy to expanded helicenes.

The primary challenge associated with syntheses of longer expanded helicenes is the required regioselective fusion of many aromatic rings. Indeed, these compounds typically possess at least twice as many rings per helical turn compared to analogues with all angular ring fusion. As a redeeming feature, however, their strain energy is relatively small.^{30,38} The first studies on expanded helicenes (1, Scheme 1a) were enabled by the application of a unified metal-mediated [2 + 2 +n] cycloaddition strategy.²⁸ An important feature of this approach is the modularity of the syntheses of the oligo-(alkynyl)arylene precursors (2). Subsequently, using the

Scheme 1. Previous Cycloaddition Strategies for the Synthesis of Expanded Helicenes

(a) [2+2+n] Cycloaddition platform for synthesis of expanded helicenes (1)

(b) Site-selective [2+2+2] cycloaddition to access an alkynylated expanded [11]-helicene (11-Hel)

discovery⁴⁰ that such [2 + 2 + n] cycloadditions can occur in a site-selective fashion, a streamlined, gram-scale synthesis of alkynylated expanded [11]-helicene 11-Hel (Scheme 1b) from phenanthrene trimer 3 was developed.²⁹ This synthesis was simplified by the use of a single building block (4) that is available on a 35-40 gram scale and can be trimerized to give 3 in only two (total) steps.

Here, we show that the site selectivity associated with an Ircatalyzed [2 + 2 + 2] cycloaddition allows the iterative synthesis of a homologous series of expanded helicenes containing 15, 19, and 23 rings on the inner helical circuit. This synthetic strategy was enabled by the development of a large, highly functionalized building block (compound 9), synthesized on a multigram scale with the first iteration of the site-selective [2 + 2 + 2] reaction (Scheme 3). This building block served as a common intermediate to all three helicenes via a two-step process: (1) a modular, transition-metalmediated $C-\hat{C}$ bond formation and (2) a second iteration of the site-selective [2 + 2 + 2] reaction. Compound 23-Hel (Figure 1b) is 7 rings longer than any reported ortho-annulated carbohelicene (cf. Fujita's [16]-helicene³⁵) and 8 rings longer than the next longest expanded helicene.³⁷ For the expanded helicenes reported here, $\Delta G_{\rm e}^{\ddagger}$ increases linearly with length, at 16, 22, and 29 kcal/mol for the expanded [15]-, [19]-, and [23]-helicenes, respectively (in o-DCB solvent). The high ΔG^{\ddagger} of the [23]-helicene permitted full resolution of its enantiomers, which display |gabs| of 0.056 at 428 nm, significantly outperforming all previously reported carbohelicenes.

■ RESULTS AND DISCUSSION

Efforts to obtain longer expanded helicenes began with the synthesis of 15-Hel (Scheme 2), in a direct extension of the previous strategy used to access the analogous 11-Hel (Scheme 1b).²⁹ The cross-coupling of dimeric 5 with 2 equiv of unsymmetrical Grignard reagent 6 proceeded as expected, affording tetrameric 7 in 57% yield. A subsequent

Scheme 2. First Generation Synthesis of 15-Hel

threefold [2+2+2] cycloaddition gave the desired **15-Hel**, but in a much lower yield than for the analogous **11-Hel** (24 vs 88% by ¹H NMR spectroscopy). A well-defined side product with reduced symmetry also formed in 60% yield. Subjection of the mixture to preparatory thin layer chromatography enabled isolation of the side product, which was determined to be compound **8** by a combination of multidimensional NMR spectroscopy and matrix-assisted laser desorption/ionization (MALDI) (see page \$28 for details of structure assignment). This unusual product appears to have formed through a *fully intra*molecular [2+2+2] side reaction. While the ratio of **8** to **15-Hel** varied slightly with concentration, appreciable selectivity could not be achieved.

The low yield for 15-Hel indicated that a modified approach was required for longer analogues. Two considerations guided such modifications. First, the construction of oligomeric phenanthrene-based precursors analogous to trimeric 3 and tetrameric 7 is more difficult for longer oligomers. Second, and more importantly, the probability of fully intramolecular [2 + 2]+ 2] side reactions (like that leading to 8) is expected to increase as a function of the oligomer length. We reasoned that a larger building block (i.e., one with more fused rings) might address both of these problems. Harnessing the recently discovered⁴⁰ site selectivity of the [2 + 2 + 2] reaction, tribenzopentaphene dibromide 9 (Scheme 3) was accessed on the multi-gram scale from easily assembled phenanthrene dimer 5. This ideal building block was then transformed to its diprotio (10) and diiodo (11) derivatives via a twofold Li/Br exchange followed by a MeOH or I₂ quench, respectively.

To utilize tribenzopentaphene building blocks for the synthesis of oligomeric synthetic intermediates, symmetrical derivatives such as 9 and 11 require unsymmetrical, monofunctional analogues as capping groups in coupling reactions to achieve well-defined helicenes of precise lengths. This concept is illustrated by the efficient use of phenanthrene dibromide 4 (Scheme 1b) in a selective monolithiation via Li/Br exchange to provide large quantities of dimeric 5^{28,40} and unsymmetrical derivatives such as 6.²⁹ Unfortunately, attempts to carry out an analogous Li/Br exchange for desymmetrization of 9 yielded statistical mixtures of starting 9, desired unsymmetrical derivative 12, and doubly protiodebrominated

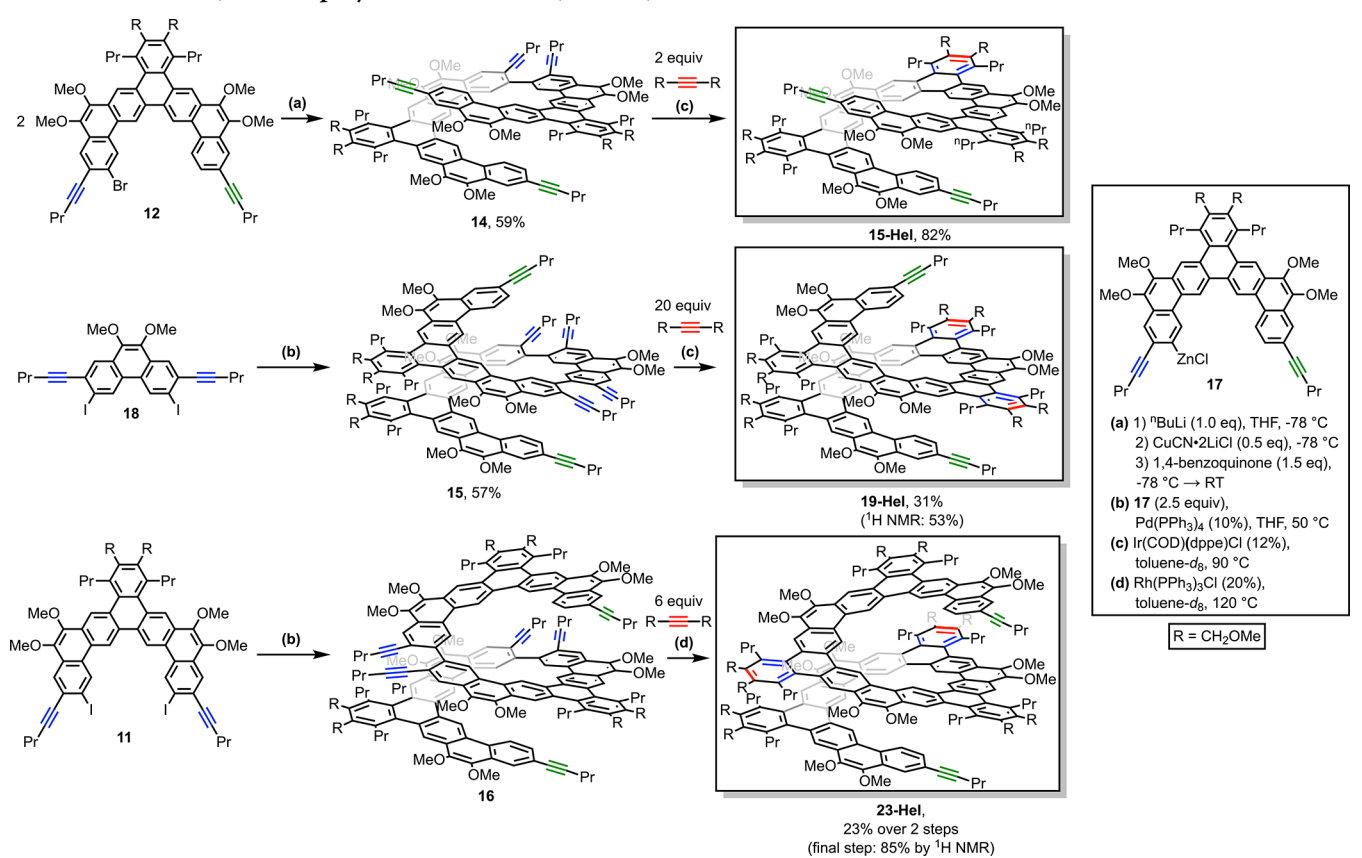
Scheme 3. Synthesis of a Large Building Block (9) and Its Symmetrical (10 and 11) and Unsymmetrical (12) Derivatives

(a) Ir[(COD)CI]₂ (1%), dppe (2%), toluene, 80 °C, 2 h; (b) ⁿBuLi (2.2 eq), THF, -78 °C, then I₂, -78 °C \rightarrow RT; (c) Pd(PPh₃)₄ (1.0 eq), benzene, 80 °C, 16 h, then DIBAL (1.5 eq)

side product **10** (after MeOH quench). Thus, an alternative strategy to leverage the spatial proximity of the two bromide substituents was pursued, with successive treatment of **9** with Pd(PPh₃)₄ (1.0 equiv) and DIBAL (1.5 equiv) to give a 1: 10: 1 mixture of **9**, **12**, and **10** (Scheme 3). Importantly, this inseparable mixture was sufficiently enriched in the desired **12** to allow a successful cross-coupling reaction (vide infra). The origin of this selectivity is likely the preferential formation of the desymmetrized, sterically encumbered intermediate **13** via a one-site oxidative addition.

The two-step syntheses of expanded helicenes 15-Hel, 19-Hel, and 23-Hel, using the derivatives of building block 9, are shown in Scheme 4. The precursor oligo(alkynyl)arylenes 14-16 were accessed in a modular fashion by homo- or crosscoupling reactions. Specifically, subjection of 12 to Iyoda/ Lipschutz CuCN-mediated homocoupling conditions^{41'} gave dimeric precursor 14 in 59% yield. Likewise, 12 was transformed in situ to the organozinc reagent 17, which then underwent a twofold Negishi cross-coupling with either phenanthrene diiodide 18 or tribenzopentaphene diiodide 11 to give trimeric precursors 15 and 16, respectively. Compound 16 could not be isolated in the pure form, but the crude material was used successfully for the next step. Precursor 14 underwent a one-site [2 + 2 + 2] reaction to furnish 15-Hel in 82% isolated yield. Importantly, the geometry of 14 makes the deleterious, fully intramolecular [2 + 2 + 2] reaction to form side product 8 (Scheme 2) infeasible. In fact, analogous side products will be geometrically infeasible for any higher homooligomers of the larger building block 9. Subjection of 15 to identical conditions gave the desired 19-Hel in 31% isolated yield (53% by ¹H NMR spectroscopy). The lower yield is accompanied by an unidentified, well-defined side product, which likely results from the presence of a phenanthrene unit in the oligomer. In contrast, 23-Hel forms in high yield (85% by ¹H NMR spectroscopy from 16). Here, Rh(PPh₃)₃Cl⁴² was found to be more effective as a precatalyst than Ir(COD)-(dppe)Cl. The isolated yield of 23-Hel was 23% (for the twostep sequence), which is reduced by the difficult (and unoptimized) cross-coupling reaction to form the precursor 16.

Scheme 4. Modular, Two-step Syntheses of 15-Hel, 19-Hel, and 23-Hel



The ¹H and ¹³C NMR spectra are consistent with the expected C2 symmetry in solution for all new helicenes, and the latter shows the two expected quaternary alkynyl resonances. Single crystals of 23-Hel were grown by slow evaporation of a CH2Cl2/hexane solution, and its molecular structure was unambiguously confirmed by single crystal X-ray diffraction (Figure 2). These syntheses served to complete a series of analogous expanded helicenes containing 11-, 15-, 19-,

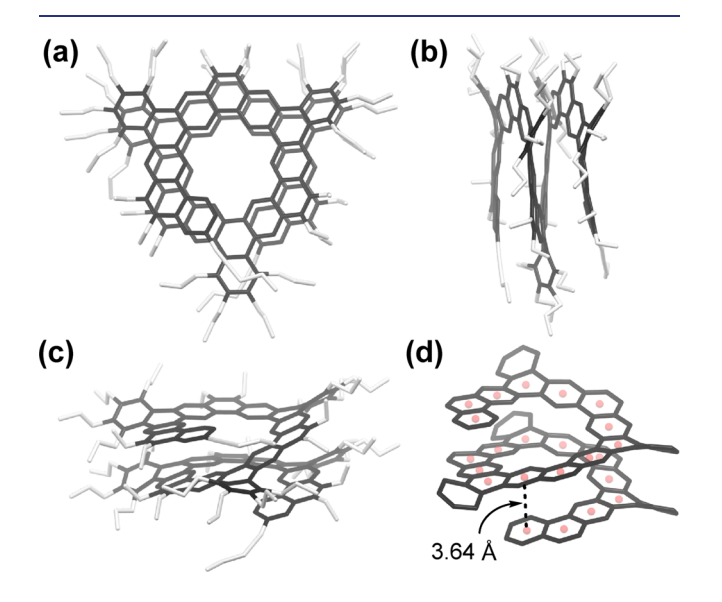


Figure 2. Molecular structure of 23-Hel as determined by single crystal X-ray diffraction: (a) top view; (b) side view; (c) front view; and (d) modified front view with truncated side chains for clarity.

and 23 rings on the inner helical circuit. Importantly, these compounds differ only in their length, presenting an ideal opportunity to probe structure-property relationships.

The structural parameters of the new helicenes were probed using a combination of X-ray crystallography (for 23-Hel) and DFT calculations at the B3LYP-D4/SVP level of theory (for all helicenes). The molecular structure of 23-Hel as determined by X-ray crystallography displays moderate (3.6–4.0 Å) intramolecular π -stacking interactions, but negligible intermolecular interactions between π -systems of adjacent molecules. The X-ray structure is in good agreement with the calculated structure (Figure S68), supporting the viability of making structural comparisons across the helicene series. Notably, with the exception of 11-Hel, diameter and helical pitch are relatively invariant to the helicene length.

The new helicenes are highly soluble in chlorinated and aromatic solvents and insoluble in more polar (e.g., MeCN and EtOH) and nonpolar (e.g., hexanes) solvents. As was previously observed for 11-Hel, 29 this apparently results from limited aggregation by π -stacking, as evidenced by the invariance of the chemical shifts in their chloroform-d 1H NMR spectra to concentration (Figures S37-S39). The limited π -stacking in solution is consistent with the absence of such interactions in the solid-state structure for 23-Hel.

Lengthening of the expanded helicene core from 11-Hel to 23-Hel is accompanied by very little change in the UV-vis absorption maxima (λ_{\max}) and onset (λ_{onset}) . The latter displays an increase from 421 to 432 nm for 11-Hel to 23-Hel, respectively, and thus a relatively unperturbed optical HOMO-LUMO gap (2.9-3.0 eV). This suggests that the effective conjugation length is relatively low in these systems.

Likewise, the emission maximum shifts by only 23 nm (from 448 to 471 nm) in the same series of compounds. These small redshifts, which are consistent with those for "classical" carbohelicenes, may result from a combination of three factors, which are difficult to deconvolute: (1) the highly benzenoid nature of the π -system; (2) the combined angular and linear ring fusion, which is analogous to cross-conjugation (e.g., in oligoenes); and (3) intramolecular interactions between π -surfaces, which become more prevalent with increasing length.

Since the primary motivation for syntheses of longer expanded helicenes was to slow enantiomerization for the isolation of enantiopure material, their ΔG_{e}^{\ddagger} were systematically determined using dynamic ¹H NMR (11-Hel and 15-Hel) or dynamic ECD (19-Hel and 23-Hel) spectroscopies (Table 1; see pages S35–S42 for details). Notably, there is a

Table 1. Summary of Experimental Enantiomerization Free Energy Barriers Determined by Dynamic ¹H NMR (11-Hel and 15-Hel) or ECD (19-Hel and 23-Hel)

compound	experimental ΔG_{e}^{\ddagger} (kcal/mol) – o-DCB solvent	experimental ΔG^{\ddagger}_{e} (kcal/mol) $-$ other solvent
11-Hel	<12	<12 (toluene- <i>d</i> ₈)
15-Hel	$15.5 \pm 0.2 \ (38 \ ^{\circ}\text{C})$	16.5 ± 0.3 (55 °C, toluene- d_8)
19-Hel	$22.9 \pm 0.1 \ (25 \ ^{\circ}\text{C})$	$24.6 \pm 0.1 \ (25 ^{\circ}\text{C}, 14\% \ \text{CH}_{2}\text{Cl}_{2} \text{ in hexanes})$
23-Hel	$29.2 \pm 0.1 \ (100 \ ^{\circ}\text{C})$	30.9 \pm 0.1 (100 °C, o-xylene)

linear relationship between $\Delta G_{\rm e}^{\ddagger}$ and the number of rings in the inner helical circuit, with the former increasing by 1.7 \pm 0.1 kcal/mol for each additional ring from 15-Hel (Figure S50). The values are 1–2 kcal/mol higher in "poorer" solvents. Importantly, the $\Delta G_{\rm e}^{\ddagger}$ for 23-Hel (29.2 \pm 0.1 kcal/mol at 100 °C in *o*-DCB) is high enough to impart configurational stability at room temperature.

Pure samples of left- (M) and right-handed (P) [23]-Hel were isolated via chiral high-performance liquid chromatography (HPLC) (Figures SS1 and SS2) and an ECD spectrum

of each was acquired in 14% CH_2Cl_2 in hexanes (Figure 3a). Optically pure 23-Hel displayed strong ECD at 428 nm ($|\Delta \varepsilon|$ = 512 M^{-1} cm⁻¹), 407 nm ($|\Delta \varepsilon|$ = 732 M^{-1} cm⁻¹), and 310 nm ($|\Delta \varepsilon|$ = 640 M^{-1} cm⁻¹). An ECD spectrum was calculated for (P)-23-Hel (with all sidechains truncated) using TD-DFT at the B3LYP-D3/6-31 + G(d,p) level of theory. It closely matched the experimental spectrum, enabling the assignment of absolute stereochemistry: like right-handed classical helicenes, (P)-23-Hel exhibits positive ECD at the absorption onset (corresponding to the red trace in Figure 3a). 23-Hel achieves a maximum $|g_{abs}|$ of 0.056 at 428 nm (Figure 3b), which is 1.7× higher than the largest previously reported ECD dissymmetry factor for a helicene-based molecule.

To investigate the origin of the exceptional chiroptical performance of 23-Hel, we first examined the effect of helical diameter on ECD dissymmetry via TD-DFT. Using the same level of theory that reproduced the ECD spectrum of 23-Hel, we calculated the largest |gabs| of three helicenes (each one ring short of a full revolution of its helix): classical [5]helicene (5-Hel-Small in the SI), truncated 11-Hel (11-Hel-Core in the SI), and a further-expanded [17]helicene (17-Hel-Wide in the SI, see page \$60 for details). For the electronic transitions with the largest $|g_{abs}|$, we observed a strong positive correlation between the magnetic dipole moment (μ_m) and the diameter of the helicene (Figure S66). Since increasing $\mu_{\rm m}$ generally increases $|g_{abs}|$, these calculations support earlier claims that increased diameter can improve chiroptical performance; however, to increase $|g_{abs}|$, the increase in μ_m must not be offset by an increase in the electric transition dipole moment (μ_e) or the unalignment of μ_m and μ_e .⁴³

Having established that $\mu_{\rm m}$ increases with the helicene diameter, we next examined the ECD dissymmetry factors for truncated versions of 11-Hel, 15-Hel, 19-Hel, and 23-Hel. These TD-DFT calculations revealed a clear trend of improved chiroptical response as a function of increasing helicene length (Figure 3c), albeit with clear saturation behavior. Visualization of the electronic transitions with the largest $|g_{\rm abs}|$ illustrates the two factors responsible for the increase in dissymmetry (Figure

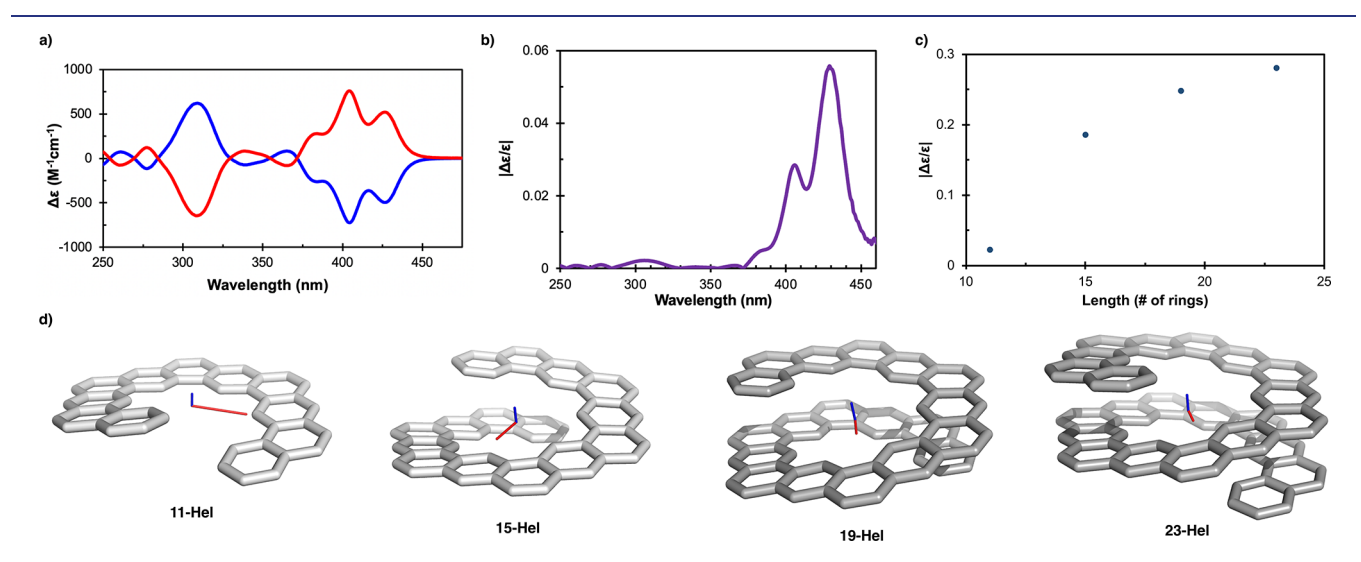


Figure 3. Chiroptical properties of expanded helicenes: (a) experimental ECD spectra of 23-Hel in 14% CH₂Cl₂ in hexanes at 25 °C; (b) experimental dissymmetry factor ($|\Delta\varepsilon/\varepsilon|$) of 23-Hel as a function of wavelength; (c) calculated maximum $|\Delta\varepsilon/\varepsilon|$ at the B3LYP-D3/6-31 + G(d,p) level as a function of the number of rings in the inner circuit of the expanded helicene; (d) visualization of calculated electronic (red) and magnetic (blue, 10× magnified for visualization) dipole moments for the electronic transition displaying the largest absolute dissymmetry factor of 11-Hel (θ = 104°), 15-Hel (θ = 130°), 19-Hel (θ = 164°), and 23-Hel (θ = 170°). Peripheral benzannulation on the helicenes has been truncated for clarity.

3d): an improved alignment of $\mu_{\rm m}$ and $\mu_{\rm e}$ (from 104° in 11-Hel to 170° in 23-Hel) and a decrease in μ_e (from 3.6 × 10⁻¹⁸ erg/cm in 11-Hel to 0.82×10^{-18} erg/cm in 23-Hel). Taken together, these computational results suggest that both the expanded diameter and increased length of 23-Hel are responsible for its high ECD dissymmetry factor, providing potential design rules to further improve chiroptical perform-

CONCLUSIONS

This report demonstrates that the elongation of expanded helicenes is an effective strategy for the isolation of configurationally stable enantiomers at room temperature. More importantly, it has been shown that the combined expansion and elongation of the classical helicene core leads to drastic improvements in chiroptical performance, with [23]-Hel displaying a near-twofold increase in ECD dissymmetry factor relative to previously reported helicene-based molecules. These results confirm previous theoretical predictions and point the way forward for designing higher-performing chiroptical materials. More generally, the iterative synthetic strategy developed here, enabled by the site selectivity of the ladder-forming [2 + 2 + 2] reaction, should be broadly applicable to structurally diverse nanocarbons.

ASSOCIATED CONTENT

Supporting Information

The Supporting Information is available free of charge at https://pubs.acs.org/doi/10.1021/jacs.2c09555.

> Experimental procedures and characterization data for all new compounds (PDF)

Accession Codes

CCDC 2195412 contains the supplementary crystallographic data for this paper. These data can be obtained free of charge via www.ccdc.cam.ac.uk/data_request/cif, or by emailing data_request@ccdc.cam.ac.uk, or by contacting The Cambridge Crystallographic Data Centre, 12 Union Road, Cambridge CB2 1EZ, UK; fax: +44 1223 336033.

AUTHOR INFORMATION

Corresponding Author

T. Don Tilley - Department of Chemistry, University of California, Berkeley, Berkeley, California 94720, United States; orcid.org/0000-0002-6671-9099; Email: tdtilley@berkeley.edu

Authors

Gavin R. Kiel - Department of Chemistry, University of California, Berkeley, Berkeley, California 94720, United

Harrison M. Bergman – Department of Chemistry, University of California, Berkeley, Berkeley, California 94720, United States; orcid.org/0000-0001-6482-2837

Adrian E. Samkian - Department of Chemistry, University of California, Berkeley, Berkeley, California 94720, United

Nathaniel J. Schuster - Department of Chemistry, Columbia University, New York, New York 10027, United States

Rex C. Handford - Department of Chemistry, University of California, Berkeley, Berkeley, California 94720, United States; orcid.org/0000-0002-3693-1697

August J. Rothenberger – Department of Chemistry, University of California, Berkeley, Berkeley, California 94720, United States

Rafael Gomez-Bombarelli — Department of Materials Science and Engineering, Massachusetts Institute of Technology, Cambridge, Massachusetts 02139, United States; orcid.org/0000-0002-9495-8599

Colin Nuckolls – Department of Chemistry, Columbia University, New York, New York 10027, United States; orcid.org/0000-0002-0384-5493

Complete contact information is available at: https://pubs.acs.org/10.1021/jacs.2c09555

Author Contributions

G.R.K. and H.M.B. contributed equally to this work.

Funding

This work was funded by the National Science Foundation under Grant No. CHE-2103696.

The authors declare no competing financial interest.

ACKNOWLEDGMENTS

Crystallographic analysis of compound 23-Hel was performed at The Advanced Light Source, which is supported by the Director, Office of Science, Office of Basic Energy Sciences, of the U.S. Department of Energy under Contract No. DE-AC02-05CH11231. We thank UC Berkeley's NMR facility for resources provided and the staff for their assistance. Instruments in the NMR facility are supported in part by NIH S10OD024998. The CD spectra were measured at the Precision Biomolecular Characterization Facility (PBCF) at Columbia University. The PBCF was made possible by funding from the U.S. National Institutes of Health under award no. 1S10OD025102-01. We thank Dr. Jia Ma for his management of the PBCF. We thank Edward Miller for the initial analytical chiral HPLC measurements that motivated further efforts.

REFERENCES

- (1) Martin, R. H. The Helicenes. Angew. Chem. Int. Ed. 1974, 13,
- (2) Shen, Y.; Chen, C.-F. Helicenes: Synthesis and Applications. Chem. Rev. 2012, 112, 1463-1535.
- (3) Gingras, M. One Hundred Years of Helicene Chemistry. Part 1: Non-Stereoselective Syntheses of Carbohelicenes. Chem. Soc. Rev. 2013, 42, 968-1006.
- (4) Gingras, M.; Félix, G.; Peresutti, R. One Hundred Years of Helicene Chemistry. Part 2: Stereoselective Syntheses and Chiral Separations of Carbohelicenes. Chem. Soc. Rev. 2013, 42, 1007-1050.
- (5) Gingras, M. One Hundred Years of Helicene Chemistry. Part 3: Applications and Properties of Carbohelicenes. Chem. Soc. Rev. 2013, 42, 1051-1095.
- (6) Barnett, L.; Ho, D. M.; Baldridge, K. K.; Pascal, R. A. The Structure of Hexabenzotriphenylene and the Problem of Overcrowded "D3h" Polycyclic Aromatic Compounds. J. Am. Chem. Soc. 1999, 121, 727-733.
- (7) Wang, X.-Y.; Wang, X.-C.; Narita, A.; Wagner, M.; Cao, X.-Y.; Feng, X.; Müllen, K. Synthesis, Structure, and Chiroptical Properties of a Double [7] Heterohelicene. J. Am. Chem. Soc. 2016, 138, 12783-
- (8) Fujikawa, T.; Segawa, Y.; Itami, K. Synthesis, Structures, and Properties of π -Extended Double Helicene: A Combination of Planar and Nonplanar π -Systems. J. Am. Chem. Soc. 2015, 137, 7763–7768.

- (9) Pradhan, A.; Dechambenoit, P.; Bock, H.; Durola, F. Fused Helicene Chains: Towards Twisted Graphene Nanoribbons. *Chem. Eur. J.* **2016**, 22, 18227–18235.
- (10) Hu, Y.; Wang, X.-Y.; Peng, P.-X.; Wang, X.-C.; Cao, X.-Y.; Feng, X.; Müllen, K.; Narita, A. Benzo-Fused Double [7]-Carbohelicene: Synthesis, Structures, and Physicochemical Properties. *Angew. Chem., Int. Ed.* **2017**, *56*, 3374–3378.
- (11) Hosokawa, T.; Takahashi, Y.; Matsushima, T.; Watanabe, S.; Kikkawa, S.; Azumaya, I.; Tsurusaki, A.; Kamikawa, K. Synthesis, Structures, and Properties of Hexapole Helicenes: Assembling Six [5]Helicene Substructures into Highly Twisted Aromatic Systems. J. Am. Chem. Soc. 2017, 139, 18512–18521.
- (12) Ball, M.; Zhong, Y.; Wu, Y.; Schenck, C.; Ng, F.; Steigerwald, M.; Xiao, S.; Nuckolls, C. Contorted Polycyclic Aromatics. *Acc. Chem. Res.* 2015, 48, 267–276.
- (13) Li, C.; Yang, Y.; Miao, Q. Recent Progress in Chemistry of Multiple Helicenes. *Chem. Asian J.* **2018**, *13*, 884–894.
- (14) Wu, Y. F.; Zhang, L.; Zhang, Q.; Xie, S. Y.; Zhang, L. S. Multiple [n]Helicenes with Various Aromatic Cores. *Org. Chem. Front.* **2022**, *9*, 4726.
- (15) Field, J. E.; Muller, G.; Riehl, J. P.; Venkataraman, D. Circularly Polarized Luminescence from Bridged Triarylamine Helicenes. *J. Am. Chem. Soc.* **2003**, *125*, 11808–11809.
- (16) Brandt, J. R.; Wang, X.; Yang, Y.; Campbell, A. J.; Fuchter, M. J. Circularly Polarized Phosphorescent Electroluminescence with a High Dissymmetry Factor from PHOLEDs Based on a Platinahelicene. *J. Am. Chem. Soc.* **2016**, *138*, 9743–9746.
- (17) Tanaka, H.; Inoue, Y.; Mori, T. Circularly Polarized Luminescence and Circular Dichroisms in Small Organic Molecules: Correlation between Excitation and Emission Dissymmetry Factors. *ChemPhotoChem* **2018**, 2, 386–402.
- (18) Xiao, X.; Pedersen, S. K.; Aranda, D.; Yang, J.; Wiscons, R. A.; Pittelkow, M.; Steigerwald, M. L.; Santoro, F.; Schuster, N. J.; Nuckolls, C. Chirality Amplified: Long, Discrete Helicene Nanoribbons. J. Am. Chem. Soc. 2021, 143, 983–991.
- (19) Li, K. J.; Chen, X. Y.; Guo, Y. L.; Wang, X. C.; Sue, A. C. H.; Cao, X. Y.; Wang, X. Y. N-Embedded Double Hetero[7]Helicenes with Strong Chiroptical Responses in the Visible Light Region. *J. Am. Chem. Soc.* **2021**, *143*, 17958–17963.
- (20) Verbiest, T.; Elshocht, S. V.; Kauranen, M.; Hellemans, L.; Snauwaert, J.; Nuckolls, C.; Katz, T. J.; Persoons, A. Strong Enhancement of Nonlinear Optical Properties Through Supramolecular Chirality. *Science* 1998, 282, 913–915.
- (21) Nuckolls, C.; Katz, T. J.; Castellanos, L. Aggregation of Conjugated Helical Molecules. *J. Am. Chem. Soc.* **1996**, *118*, 3767–3768.
- (22) Shcherbina, M. A.; Zeng, X.; Tadjiev, T.; Ungar, G.; Eichhorn, S. H.; Phillips, K. E. S.; Katz, T. J. Hollow Six-Stranded Helical Columns of a Helicene. *Angew. Chem., Int. Ed.* **2009**, *48*, 7837–7840.
- (23) Narcis, M. J.; Takenaka, N. Helical-Chiral Small Molecules in Asymmetric Catalysis. *Eur. J. Org. Chem.* **2014**, 2014, 21–34.
- (24) Yang, Y.; da Costa, R. C.; Fuchter, M. J.; Campbell, A. J. Circularly Polarized Light Detection by a Chiral Organic Semi-conductor Transistor. *Nat. Photonics* **2013**, *7*, 634–638.
- (25) Brandt, J. R.; Salerno, F.; Fuchter, M. J. The Added Value of Small-Molecule Chirality in Technological Applications. *Nat. Rev. Chem.* **2017**, *1*, No. 0045.
- (26) Yang, Y.; Rice, B.; Shi, X.; Brandt, J.; Correa da Costa, R.; Hedley, G. J.; Smilgies, D.-M.; Frost, J. M.; Samuel, I.; Otero-de-la-Roza, A.; Johnson, E.; Jelfs, K. E.; Nelson, J.; Campbell, A. J.; Fuchter, M. J. Emergent Properties of an Organic Semiconductor Driven by Its Molecular Chirality. *ACS Nano* 2017, 11, 8329–8338.
- (27) Vacek, J.; Chocholoušová, J. V.; Stará, I. G.; Starý, I.; Dubi, Y. Mechanical Tuning of Conductance and Thermopower in Helicene Molecular Junctions. *Nanoscale* **2015**, *7*, 8793–8802.
- (28) Kiel, G. R.; Patel, S. C.; Smith, P. W.; Levine, D. S.; Tilley, T. D. Expanded Helicenes: A General Synthetic Strategy and Remarkable Supramolecular and Solid-State Behavior. *J. Am. Chem. Soc.* 2017, 139, 18456–18459.

- (29) Kiel, G. R.; Bay, K. L.; Samkian, A. E.; Schuster, N. J.; Lin, J. B.; Handford, R. C.; Nuckolls, C.; Houk, K. N.; Tilley, T. D. Expanded Helicenes as Synthons for Chiral Macrocyclic Nanocarbons. *J. Am. Chem. Soc.* **2020**, *142*, 11084–11091.
- (30) Nakakuki, Y.; Hirose, T.; Matsuda, K. Synthesis of a Helical Analogue of Kekulene: A Flexible π -Expanded Helicene with Large Helical Diameter Acting as a Soft Molecular Spring. *J. Am. Chem. Soc.* **2018**, *140*, 15461–15469.
- (31) Fujise, K.; Tsurumaki, E.; Fukuhara, G.; Hara, N.; Imai, Y.; Toyota, S. Multiple Fused Anthracenes as Helical Polycyclic Aromatic Hydrocarbon Motif for Chiroptical Performance Enhancement. *Chem. Asian J.* **2020**, *15*, 2456–2461.
- (32) Zheng, W.; Ikai, T.; Yashima, E. Consecutively Fused Single-Double-, and Triple-Expanded Helicenes. *Nat. Sci.* **2022**, 2, No. e20210047.
- (33) Suarez-Pantiga, S.; Redero, P.; Aniban, X.; Simon, M.; Golz, C.; Mata, R. A.; Alcarazo, M. In-Fjord Substitution in Expanded Helicenes: Effects of the Insert on the Inversion Barrier and Helical Pitch. *Chem. Eur. J.* **2021**, *27*, 13358–13366.
- (34) Newman, M. S.; Lednicer, D. The Synthesis and Resolution of Hexahelicene. J. Am. Chem. Soc. 1956, 78, 4765–4770.
- (35) Mori, K.; Murase, T.; Fujita, M. One-Step Synthesis of [16] Helicene. *Angew. Chem., Int. Ed.* **2015**, *54*, 6847–6851.
- (36) Martin, R. H.; Baes, M. Helicenes: Photosyntheses of [11], [12] and [14]Helicene. *Tetrahedron* 1975, 31, 2135–2137.
- (37) Fujise, K.; Tsurumaki, E.; Wakamatsu, K.; Toyota, S. Construction of Helical Structures with Multiple Fused Anthracenes: Structures and Properties of Long Expanded Helicenes. *Chem. Eur. J.* **2021**, *27*, 4548–4552.
- (38) Rempala, P.; King, B. T. Simulation of Actuation by Polymeric Polyelectrolyte Helicenes. *J. Chem. Theory Comput.* **2006**, *2*, 1112–1118.
- (39) Bonifacio, M. C. Towards Polymeric Helicenes: The Chemistry of Poly(Divinyl-m-Phenylene)s; Ph.D., University of Nevada: Reno, United States -- Nevada, 2007.
- (40) Kiel, G. R.; Bergman, H. M.; Tilley, T. D. Site-Selective [2 + 2 + n] Cycloadditions for Rapid, Scalable Access to Alkynylated Polycyclic Aromatic Hydrocarbons. *Chem. Sci.* **2020**, *11*, 3028–3035.
- (41) Miyake, Y.; Wu, M.; Rahman, M. J.; Kuwatani, Y.; Iyoda, M. Efficient Construction of Biaryls and Macrocyclic Cyclophanes via Electron-Transfer Oxidation of Lipschutz Cuprates. *J. Org. Chem.* **2006**, *71*, 6110–6117.
- (42) Grigg, R.; Scott, R.; Stevenson, P. Rhodium Catalysed [2+2+2] Cycloadditions of Acetylenes. *Tetrahedron Lett.* **1982**, 23, 2691–2692.
- (43) Greenfield, J. L.; Wade, J.; Brandt, J. R.; Shi, X.; Penfold, T. J.; Fuchter, M. J. Pathways to Increase the Dissymmetry in the Interaction of Chiral Light and Chiral Molecules. *Chem. Sci.* **2021**, 12, 8589–8602.
- (44) Samkian, A. E.; Kiel, G. R.; Jones, C. G.; Bergman, H. M.; Oktawiec, J.; Nelson, H. M.; Tilley, T. D. Elucidation of Diverse Solid-State Packing in a Family of Electron-Deficient Expanded Helicenes via Microcrystal Electron Diffraction (MicroED)**. Angew. Chem. Int. Ed. 2021, 60, 2493–2499.